N82 32535

PPM Demodulation for Reed-Solomon Decoding for the Optical Space Channel

D. Divsalar, R. M. Gagliardi, and J. H. Yuen
Communications Systems Research Section

Optical communications over space channels (satellite-to-satellite or deep-space-to-relay-satellite) are commonly designed as pulse-position-modulated (PPM) laser links. When coding is needed to improve the link performance, it is advantageous to use Reed-Solomon (RS) block codes over the PPM frames to obtain the largest degree of error correction. Since RS codes can correct both symbol errors and symbol erasures, a question arises as to the best way to demodulate the PPM laser fields in order to generate the input symbols for the RS decoder. The method selected for demodulating (converting the received laser field to digital symbols) will define the erasure and transmitted symbols of the laser link, and therefore will determine the word error probabilities of the system. In this paper, several possible demodulating schemes were considered, and the effect of each on RS decoding performance was computed. This computation was carried out for various optical receiver models, and required fairly lengthy numerical analysis to determine accurate word error probabilities when the RS code lengths are long. It is shown that simple threshold decisioning of pulse slots will produce performance that degrades as the background noise increases. This is caused by the generation of too many erasures for the RS decoder to handle. We propose a decision scheme, delta-max demodulation, which offers improvement over threshold decisioning by redefining the generation of an erasure.

I. Introduction

In this paper we study the M-ary optical pulse-position-modulation (PPM) communication system shown in Fig. 1. Source bits are encoded into channel symbols from an M-ary alphabet, which are used to generate a PPM laser pulse sequence. The optical pulse is transmitted to the optical receiver and photodetected. The photodetector produces random count variables for each slot corresponding to a PPM frame. The count variables are converted back to channel symbols for the Reed-Solomon (RS) decoder. The latter provides error correction capability for decoding the source bits.

A question arises as to how the observed photodetected counts should be converted to channel symbols so as to obtain the best RS decoding performance. This report addresses this question.

If no RS encoding is used (the source bits are directly blocked into PPM symbols), maximum likelihood decoding, using the counts as observables, requires a maximum count selection for each PPM frame, with a random choice among any count ties (more than one maximum count). If the resulting error probability is not low enough, coding must be used

to improve performance, with the source bits first encoded into channel words, then the words sent as PPM pulses. When coding is inserted, it is no longer obvious that the maximum likelihood frame decisioning is optimal, since it does not allow for channel symbol erasures. When background noise is negligible, it has been argued (Refs. 1, 2) that matched RS coding appears as a natural encoding scheme, since only channel erasures can occur, and RS decoding has maximal capability for correcting erasures. The RS code size is selected to match the PPM frame size (channel alphabet size) and maximum count demodulation is used, with all ties interpreted as erasures. In the noiseless case, an erasure can occur only if a PPM signaling slot produces no counts.

When background noise is present, conversion of counts to channel symbols will involve errors as well as erasures. The number of erasures that will occur will depend on how the conversion defines an erasure. Since RS decoding can correct more erasures than errors, a question then arises in determining the best way to allocate erasures and errors by proper selection of the conversion rule. In the following sections we examine several conversion algorithms and the resultant performance of each when operating with background noise and RS decoding. This performance will depend on the model of the photodetector used in the optical detection receiver. If a high gain, ideal photomultiplier tube is assumed for the photodetection, the count variables are Poisson distributed with mean values dependent on the received field during that slot. If a high-gain random photodetector is assumed, the counts are more nearly discrete-Gaussian distributed, centered around the mean multiplied count, with a variance dependent on the detector excess noise factor. In each case the postdetection thermal noise can be neglected.

II. Count-Symbol Conversion Rules

In this study we consider two different methods for converting the observed photodetected counts to channel symbols and erasures. The methods differ primarily in the way a symbol decision is made and the way in which an erasure is defined. The methods are labeled as threshold demodulation and delta-max (δ-max) demodulation. In threshold demodulation a threshold γ is set, and any count above γ is called a pulse and a count below γ is called a zero. A symbol decision is made *only if* a single pulse occurs in a PPM frame, selecting the symbol corresponding to the pulse location. All other situations are defined as an erasure. This sequence of frame decisions is then fed into the RS decoder. In δ-max demodulation, a symbol is selected only if no other count is within δ of the maximum count. Otherwise an erasure is declared. Note that both these methods have the advantage that the number of erasures can be controlled by adjustment of the parameters γ and δ.

III. Poisson Counting, δ-Max Demodulation

Consider a Poisson count model and δ-max demodulation for generating the RS symbols. In optical PPM communication, every $\log_2 M$ binary data bits are transmitted by placing an optical light pulse in one of the M designated pulse slots. M slots constitute a PPM frame (Ref. 3). Thus each pulse represents a symbol, depending on its pulse slot location. These $\log_2 M$ binary bits therefore correspond to a Reed-Solomon (RS) symbol. At the PPM optical receiver, a photodetector counts the number of photons in each slot. Let the M photon counts $\{n_i\}_{i=1}^{M}$ correspond to the M time slots. Let n be a vector with dimension M with elements n_i. Then the probability of receiving n given a pulse is sent in jth time slot is (note n_i's are independent Poisson distributed random variables)

$$p(n|s_j) = \frac{(K_s + K_b)^{n_j}}{n_j!} e^{-(K_s + K_b)} \prod_{\substack{i=1 \\ i \neq j}}^{M} \frac{(K_b)^{n_i}}{n_i!} e^{-K_b} \quad (1)$$

where K_s is the average number of received photons per PPM frame and K_b is the average number of background noise photons per slot. We notice that the expected number of photons we receive in the signal slot is $K_s + K_b$ and the expected number of photons in other slots each is K_b. We set a level $\Delta \geq 1$ and we make a tentative decision for signal send in the jth slot if for some j

$$\frac{p(n|s_j)}{p(n|s_i)} > \Delta \quad \forall i \neq j \quad (2)$$

and make no tentative decision (erasure) otherwise. Equation (2) is equivalent to

$$\ln p(n|s_j) > \ln \Delta + \ln p(n|s_i) \quad \forall i \neq j \quad (3)$$

Redefine

$$\Delta = \left(\frac{K_s + K_b}{K_b}\right)^{\delta} \quad (4)$$

for some $\delta \geq 0$. Then using (1) in (3) we get equivalently

$$n_j > \delta + n_i \quad \forall i \neq j \quad (5)$$

Hence the maximum count test in (5) is equivalent to testing if the likelihood ratio in (2) is suitably large. The corresponding demodulator structure is shown in Fig. 2, with decision rule given in (5).

We wish to find expressions for the probability of correct detection of transmitted signal P_C, the probability of incorrect detection of transmitted signal P_S, and the probability of no tentative decision (erasure) P_E. We will correctly detect the true signal slot j corresponding to transmitted laser pulse s_j, if (5) is true. The probability of this occurring is

$$P_C = Pr \{n_j > n_1 + \delta, n_j > n_2 + \delta, \ldots, n_j > n_{j-1} + \delta,$$

$$n_j > n_{j+1} + \delta, \ldots, |s_j\}$$

$$= \sum_{k=\delta+1}^{\infty} Pr \{n_i < k - \delta \ \forall \ i \neq j | s_j\} \ Pr \{n_j = k | s_j\}$$

$$= \sum_{k=\delta+1}^{\infty} \left[\sum_{i=0}^{k-\delta-1} Pos(i, K_b) \right]^{M-1} Pos(k, K_s + K_b) \quad (6)$$

where

$$Pos(i, \lambda) = \frac{\lambda^i}{i!} e^{-\lambda} \quad (7)$$

By change of variable we get

$$P_C = \sum_{k=0}^{\infty} \left[\sum_{i=0}^{k} Pos(i, K_b) \right]^{M-1} Pos(k + \delta + 1, K_s + K_b) \quad (8)$$

On the other hand we make an incorrect decision if for a given transmitted pulse in jth time slot, for any $i \neq j$, we have

$$n_i > n_m + \delta \ \forall \ m \neq i \quad (9)$$

Then

$$P_S = Pr \{n_i > n_m + \delta \ \forall \ m \neq i, \text{ any } i \neq j | s_j\}$$

$$= (M - 1) \sum_{k=\delta+1}^{\infty} Pr \{n_m < k - \delta \ \forall \ m \neq i | s_j\} Pr \{n_i = k | s_j\}$$

$$= (M - 1) \sum_{k=\delta+1}^{\infty} \left[\sum_{i=0}^{k-\delta-1} Pos(i, K_b) \right]^{M-2}$$

$$\cdot \left[\sum_{i=0}^{k-\delta-1} Pos(i, K_s + K_b) \right] \cdot Pos(k, K_b) \quad (10)$$

By change of variable we get

$$P_S = (M - 1) \sum_{k=0}^{\infty} \left[\sum_{i=0}^{k} Pos(i, K_b) \right]^{M-2}$$

$$\left[\sum_{i=0}^{k} Pos(i, K_s + K_b) \right] \cdot Pos(k + \delta + 1, K_b) \quad (11)$$

Clearly the probability of no tentative decision (probability of erasure) is

$$P_E = 1 - P_C - P_S \quad (12)$$

A Reed-Solomon code of code block $N = M - 1$ and information block K can produce a correct code word if s the number of decoder input symbol errors and e the number of decoder input symbol erasures satisfy the following relation

$$2s + e < N - K + 1 \quad (13)$$

From this relation we note that the RS code can correct twice the number of erasures than the number of symbol errors. It is for this reason that we have tried to introduce some soft decisions at the demodulator in order to produce more erasures. Of course, if we expand the region of no hard decisions in the decision region by too large an amount, the number of erasures will increase in a given block code, and the RS decoder will not be able to correct them.

For the RS code three events may occur. The first event occurs if the number of error and erasure symbols satisfies (13), for which the decoder can correctly decode the code word, and therefore the information block. The second event occurs when (13) is not satisfied, and the combination of symbol errors and symbol erasures is such that the received code block resembles a code signal other than the transmitted one (i.e., the received code block is closer to some other code signal than the transmitted code signal).

In this second event the decoder errs, and gives an incorrect decoded code word. The third event is a complement of the two above events. In this third event, the decoder fails to decode and produces the undecoded channel symbols and randomly decides on erasures. For large M the probability of the second event, for the practical range of interest is usually very small and can be ignored. The probability that the incorrect code word is selected by the decoder, P_w(RS), is (Ref. 4)

$$P_w(RS) = \sum_{s=0}^{N} \sum_{e=q}^{N-s} \binom{N}{s}\binom{N-s}{e} P_S^s P_E^e P_C^{N-s-e} \quad (14)$$

where

$$q = max\,(N - K + 1 - 2s, 0) \quad (15)$$

and the bit error probability $P_b(RS)$ is

$$P_b(RS) = \frac{M}{2(M-1)} \sum_{s=0}^{N} \sum_{e=q}^{N-s} \binom{N}{s}\binom{N-s}{e}\left(\frac{s+e}{N}\right)$$

$$\cdot P_S^s P_E^e P_C^{N-s-e} \quad (16)$$

Equation (16) has been numerically evaluated for the Poisson channel. We considered three classes of RS codes: the (255,127) code with code rate 1/2, the (255,191) code with code rate 3/4, and the (255,223) code with code rate 7/8. These codes are matched to a PPM frame with $M = 256$ slots. For each case we plotted $P_b(RS)$ in (16) versus K_s for various K_b and several values of δ. The results are shown in Figs. 3 through 8. We see that the performance degrades as the noise count K_b increases and as the correction capability of the RS code decreases. In addition, performance is uniformly improved as δ is decreased, with best performance occurring at $\delta = 0$. This corresponds to a maximum likelihood decision on each PPM frame with all maximum ties denoted as erasures. In other words, there appears to be no advantage in widening the erasure definition for these parameter values.

IV. Poisson Counting, Threshold Demodulation

PPM threshold demodulation with Reed-Solomon decoding has been studied for the case of extremely low background noise[1] and thermal noise (Ref. 4). Here we examine the high-gain photodetector case so that the Poisson Counting Process is a valid model. In threshold demodulation, we set a threshold γ and count the number of received photons in each slot. We then compare each number with γ: if it exceeds γ, we claim signal detection in that time slot. If it does not, we claim noise detection in that time slot. We can detect the transmitted signal correctly only if in one of the slots the number of photons exceeds γ, while in all other slots it does not. Then if P_{ds} denotes the probability of signal detection in a time slot, and P_{dn} denotes the probability of correct detection of noise

---

[1]Only dark current was assumed in Ref. 4 and can be treated as extremely low background noise.

in a time slot, the probability of correct PPM signal detection is

$$P_C = P_{ds} P_{dn}^{M-1} \quad (17)$$

The probability of incorrect detection is

$$P_S = (M - 1)(1 - P_{ds})(1 - P_{dn}) P_{dn}^{M-2} \quad (18)$$

and the probability of erasure is

$$P_E = 1 - P_C - P_S \quad (19)$$

For the Poisson channel

$$P_{ds} = \sum_{k=\gamma+1}^{\infty} \frac{(K_s + K_b)^k}{k!} e^{-(K_s + K_b)} \quad (20)$$

$$P_{dn} = \sum_{k=0}^{\gamma} \frac{(K_b)^k}{k!} e^{-K_b} \quad (21)$$

Equations (17)–(21) can again be used in (16) to evaluate performance. The numerical computation has been carried out for the same code and count parameters as in the previous section, and the results superimposed in Figs. 3 to 8. The thresholds were set at $\gamma = 1$ and 2 counts, while $\gamma = 0$ corresponds to no threshold (any observed count was considered a pulse). We see that performance with threshold demodulation also degrades with noise count and decreasing code capability, but is much more sensitive to noise levels. In particular we note a severe degradation when no threshold is used and the noise increases from 10^{-4} to 10^{-3} counts. Note that in all cases the δ-max procedure, with $\delta \to 0$, is uniformly better than the threshold tests, although the two perform similarly if the noise count is low enough. Also note that in Figs. 3, 5 and 7 the optimum threshold γ changes with K_s.

V. Gaussian Counting, δ-Max Demodulation

When nonideal photodetectors are introduced, the count statistics no longer are Poisson. Although primary photoelectrons released from photoemissive surfaces are usually governed by Poisson statistics, secondary electrons generated via multianode secondary emissions, as in photomultiplier vacuum tubes or by avalanche photodetectors (APD), generally produce more symmetrical distributions. The later distributions can often be modeled by Gaussian-shaped distributions (Refs. 5, 6).

Let the PPM slot integrations generate the sequence of secondary count variables n_i, $i = 1, \ldots, M$, where the mean and variance of n_i's are as follows:

In signal slot j: $E\{n_j\} \overset{\Delta}{=} m_1 = G(K_s + K_b)$

$$\sigma_{n_j}^2 \overset{\Delta}{=} \sigma_1^2 = G^2 F(K_s + K_b) \qquad (22)$$

In noise slot i: $E\{n_i\} \overset{\Delta}{=} m_0 = GK_b$

$$\sigma_{n_i}^2 \overset{\Delta}{=} \sigma_0^2 = G^2 F K_b \qquad (23)$$

where G is the photomultiplier or APD gain and F denotes its excess noise factor.

Let n be a vector with dimension M with elements n_i. Then the probability of receiving n given that a pulse is sent in the jth time slot is

$$p(n|s_j) = \frac{c_1}{\sqrt{2\pi\sigma_1^2}} e^{\frac{-(n_j - m_1)^2}{2\sigma_1^2}} \prod_{\substack{k=1 \\ k \neq j}}^{M} \frac{c_0}{\sqrt{2\pi\sigma_0^2}} e^{\frac{-(n_k - m_0)^2}{2\sigma_0^2}} \qquad (24)$$

where c_0 and c_1 are normalization factors.

We again set a level $\Delta > 1$ and we make a tentative decision for signal sent in the jth slot if for some j

$$\frac{p(n|s_j)}{p(n|s_i)} > \Delta \quad \forall \, i \neq j \qquad (25)$$

and make no tentative decision (erasure) otherwise. Equivalently,

$$\ln p(n|s_j) > \ln\Delta + \ln p(n|s_i) \quad \forall \, i \neq j \qquad (26)$$

Redefine

$$\Delta = \exp\left[\delta(\sigma_1^2 - \sigma_0^2)/2\sigma_0^2\sigma_1^2\right] \qquad (27)$$

for some $\delta \geq 0$. Then using (24) in (26) we get equivalently

$$n_j > \sqrt{\delta + n_i^2} \qquad \forall \, i \neq j \qquad (28)$$

The corresponding demodulator structure is as shown in Fig. 2, with decision rule given in (28).

Then

$$P_C = Pr\{n_j > \sqrt{\delta + n_i^2} \quad \forall \, i \neq j | s_j\}$$

$$= \sum_{k > \sqrt{\delta}} Pr\{n_i < \sqrt{k^2 - \delta} \quad \forall \, i \neq j | s_j\} Pr\{n_j = k | s_j\}$$

$$= \sum_{k > \sqrt{\delta}} \left[\sum_{0 < i < \sqrt{k^2 - \delta}} P_0(i)\right]^{M-1} P_1(k) \qquad (29)$$

where

$$P_i(k) = \frac{c_i}{\sqrt{2\pi\sigma_i^2}} e^{\frac{-(k - m_i)^2}{2\sigma_i^2}} \; ; \quad i = 0, 1 \qquad (30)$$

and c_i is a normalization factor, such that

$$\sum_{k=0}^{\infty} P_i(k) = 1 \qquad (31)$$

Similarly

$$P_S = Pr\{n_i > \sqrt{n_m^2 + \delta} \; \forall \, m \neq i, \text{any } i \neq j | s_j\}$$

$$= (M - 1) \sum_{k > \sqrt{\delta}} \left[\sum_{0 < i < \sqrt{k^2 - \delta}} P_0(i)\right]^{M-2}$$

$$\cdot \left[\sum_{0 < i < \sqrt{k^2 - \delta}} P_1(i)\right] P_0(k) \qquad (32)$$

and finally

$$P_E = 1 - P_C - P_S \qquad (33)$$

Since G is very large for numerical computations we can approximate summations in (29) and (32) by integrations. Then we get

$$P_C = \frac{c_0^{M-1} c_1}{\sqrt{2\pi}} \int_{\frac{\sqrt{\delta}-m_1}{\sigma_1}}^{\infty} \left[1 - Q\left(\frac{m_0}{\sigma_0}\right) \right.$$

$$\left. - Q\left(\frac{\sqrt{(\sigma_1 y + m_1)^2 - \delta} - m_0}{\sigma_0}\right) \right]^{M-1} e^{-y^2/2} \, dy \qquad (34)$$

and

$$P_S = \frac{(M-1) c_0^{M-1} c_1}{\sqrt{2\pi}} \int_{\frac{\sqrt{\delta}-m_0}{\sigma_0}}^{\infty} \left[1 - Q\left(\frac{m_0}{\sigma_0}\right) \right.$$

$$- Q\left(\frac{\sqrt{(\sigma_0 z + m_0)^2 - \delta} - m_0}{\sigma_0}\right) \right]^{M-2} \left[1 - Q\left(\frac{m_1}{\sigma_1}\right) \right.$$

$$\left. - Q\left(\frac{\sqrt{(\sigma_0 z + m_0)^2 - \delta} - m_1}{\sigma_1}\right) \right] \cdot e^{-z^2/2} \, dz \qquad (35)$$

where

$$Q(x) \stackrel{\Delta}{=} \frac{1}{\sqrt{2\pi}} \int_x^{\infty} e^{-t^2/2} \, dt$$

$$= 0.5 \, \text{Erfc}(x/\sqrt{2}) \qquad (36)$$

Equation (16), with (33), (34), and (35) inserted, gives the performance for the photomultiplier or APD case. Results of the computation are shown in Figs. 9 through 11 for δ-max demodulation. Each δ-m: : curve has been optimized at each value of K_s by adjusting δ for minimal P_b (RS).

VI. Gaussian Counting, Threshold Demodulation

Here demodulator concept is the same as discussed in Section IV. We can use results of Section IV, but replacing P_{ds} and P_{dn} with

$$P_{ds} = \sum_{k=\gamma+1}^{\infty} \frac{c_1}{\sqrt{2\pi\sigma_1^2}} e^{-\frac{(k-m_1)^2}{2\sigma_1^2}} \qquad (37)$$

$$P_{dn} = \sum_{k=0}^{\gamma} \frac{c_0}{\sqrt{2\pi\sigma_0^2}} e^{-\frac{(k-m_0)^2}{2\sigma_0^2}} \qquad (38)$$

Again approximating summations by integrations we get

$$P_{ds} = Q\left(\frac{\gamma - m_1}{\sigma_1}\right) c_1 \qquad (39)$$

and

$$P_{dn} = \left[1 - Q\left(\frac{m_0}{\sigma_0}\right) - Q\left(\frac{\gamma - m_0}{\sigma_0}\right) \right] c_0 \qquad (40)$$

Numerical results using (37) – (40) are included in Figs. 9 through 11. It again follows that uniformly better performance occurs with δ-max demodulation over threshold demodulation.

VII. Conclusion

This paper proposes a delta-max demodulator for Reed-Solomon coded M-ary PPM modulation over an optical communication channel. This delta-max demodulator is compared with the threshold demodulator which is currently in use. Both of these demodulators have identical performance in the absence of background noise. As the intensity of background noise increases, the delta-max demodulator outperforms the threshold demodulator. Also, the higher the code rate, the more advantage the delta-max demodulator has.

References

1. McEliece, R. J., "Practical Codes for Photon Communication," *IEEE Trans. Infor. Theory*, Vol. IT-27, No. 4, pp. 393-398, July 1981.

2. Massey, J. L., "Capacity, Cutoff Rate, and Coding for a Direct Detection Optical Channel," *IEEE Trans. Comm.*, Vol. COM-26, Nov. 1981.

3. Gagliardi, R., and Karp. S., *Optical Communications*, Wiley, 1976.

4. Lesh, J. R., Katz, J., Tan, H. H., and Zwillinger, D., "2.5-Bit/Detected Photon Demonstration Program: Analysis and Phase I Results," *TDA Progress Report 42-66*, Jet Propulsion Laboratory, Pasadena, Calif., pp. 115-132, Dec. 1981.

5. Webb, P. P., McIntyre, R. J., and Conradi, J.," Properties of Avalanche Photodiodes," *RCA Review*, Vol. 35, June 1974, pp. 234-278.

6. Sorensen, N., and Gagliardi, R., "Performance of Optical Receivers with Avalanche Photodetection," *IEEE Trans. Comm.*, Vol. COM-27, Sept. 1979.
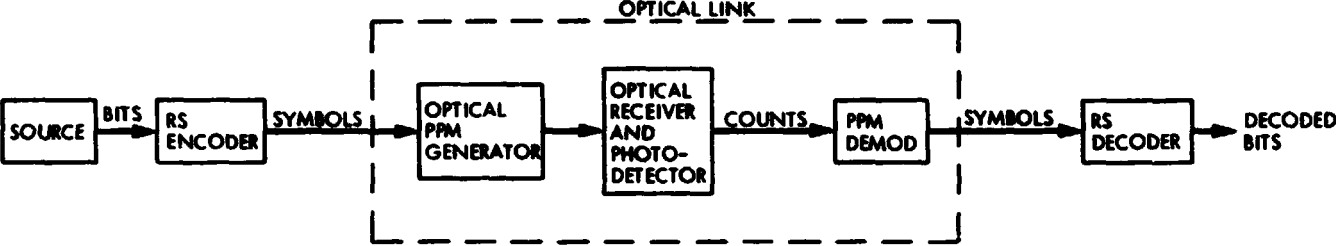
Fig. 1. PPM communication system, block diagram
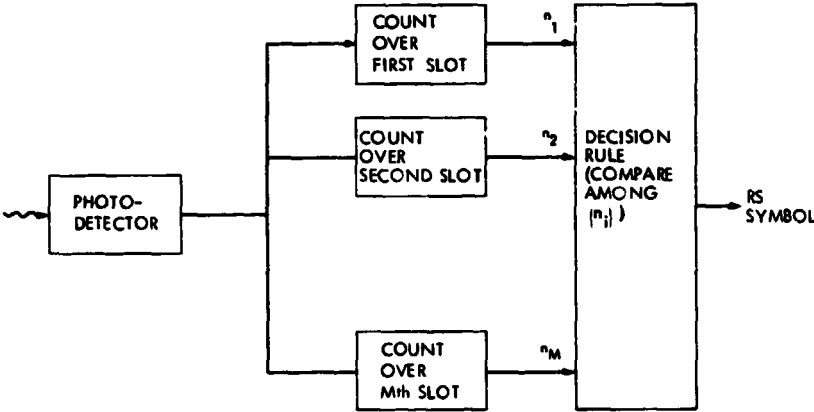
Fig. 2. Demodulator structure
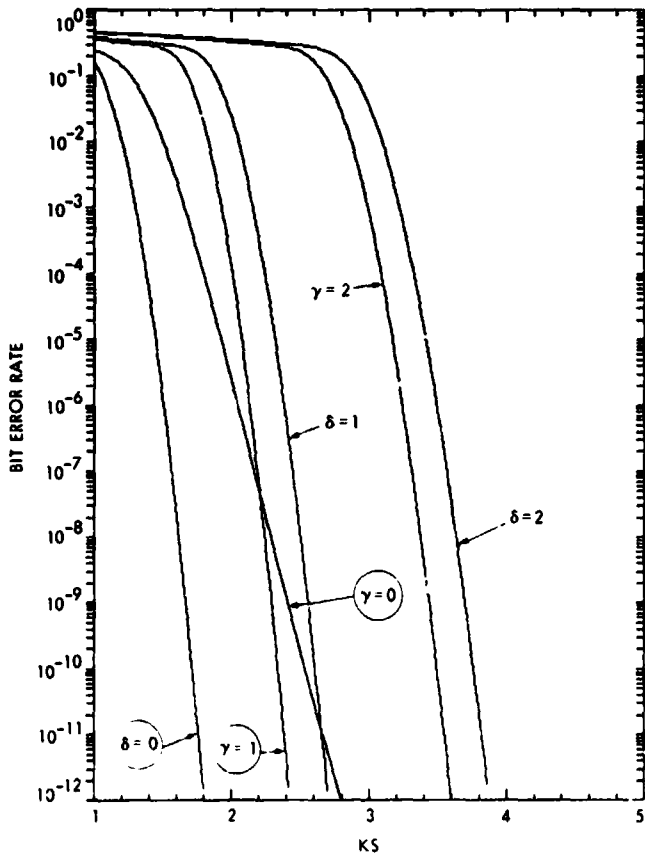
Fig. 3. Bit error rate vs K_s for $K_b = 10^{-3}$ for RS (255, 127)
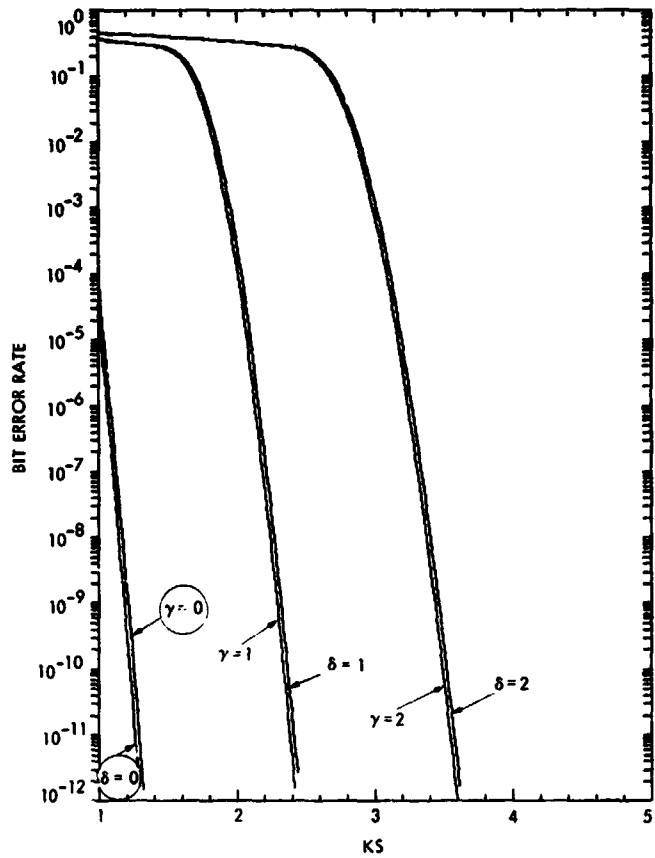
Fig. 4. Bit error rate vs K_s for $K_b = 10^{-4}$ for RS (255, 127)
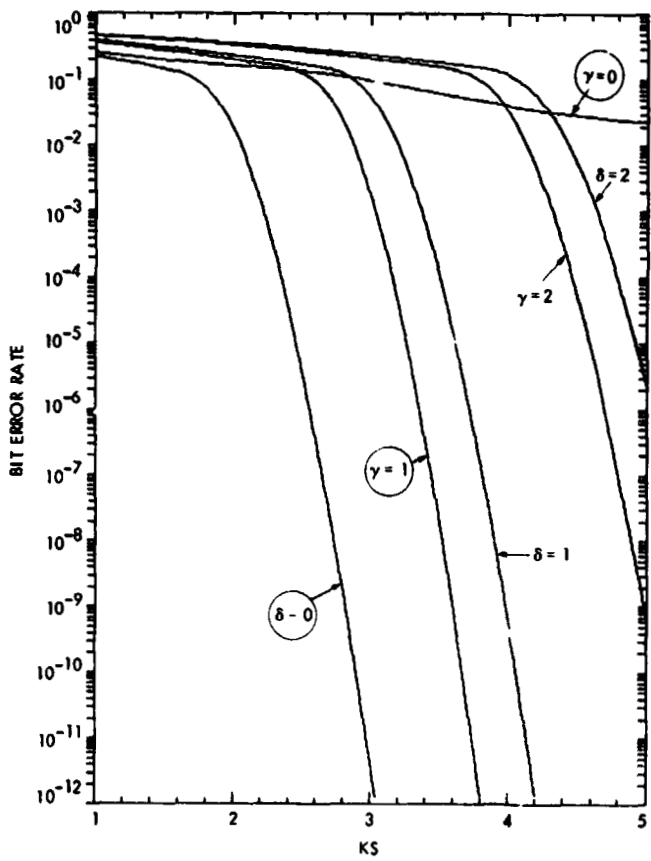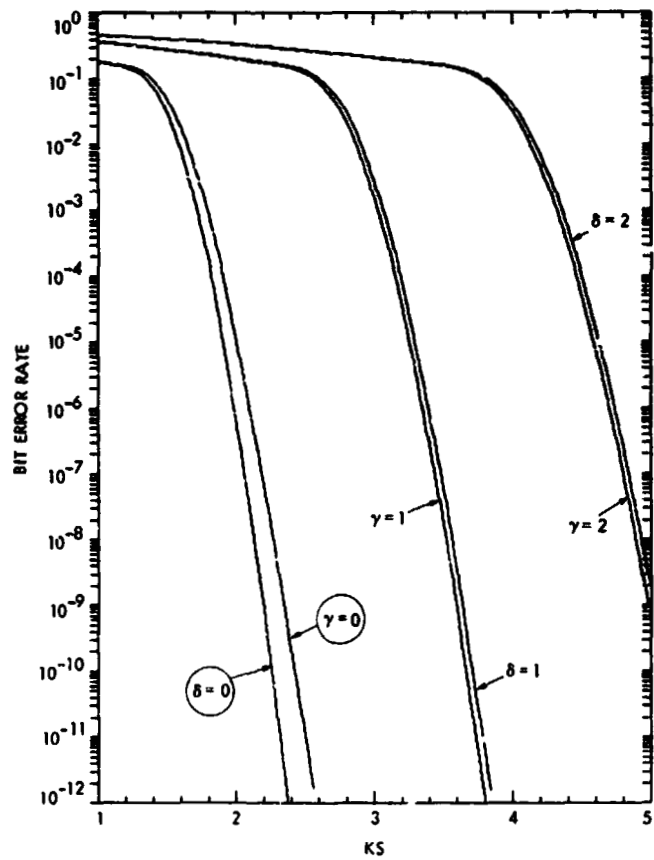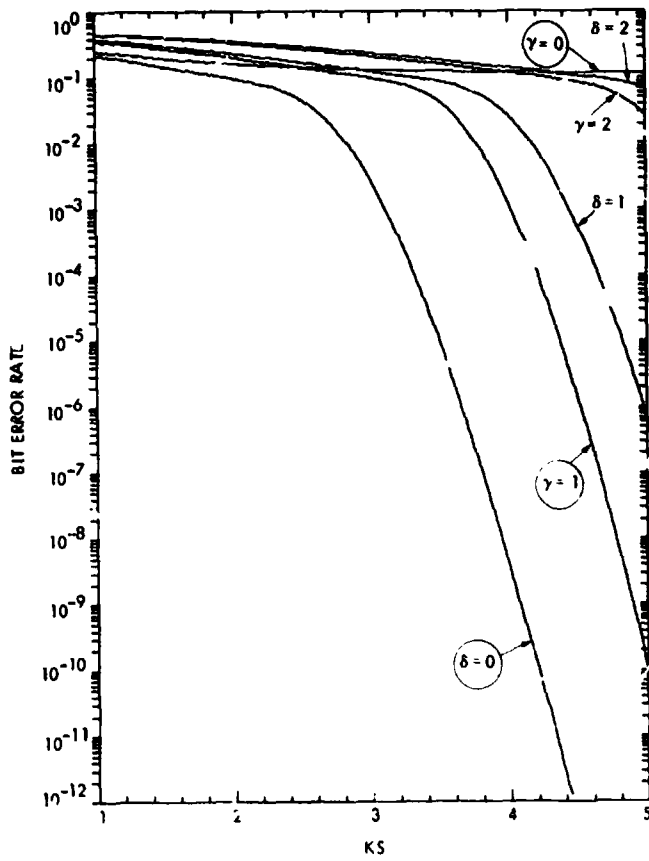
Fig. 5. Bit error rate vs K_s for $K_b = 10^{-3}$ for RS (255, 191)

Fig. 6. Bit error rate vs K_s for $K_b = 10^{-4}$ for RS (255, 191)

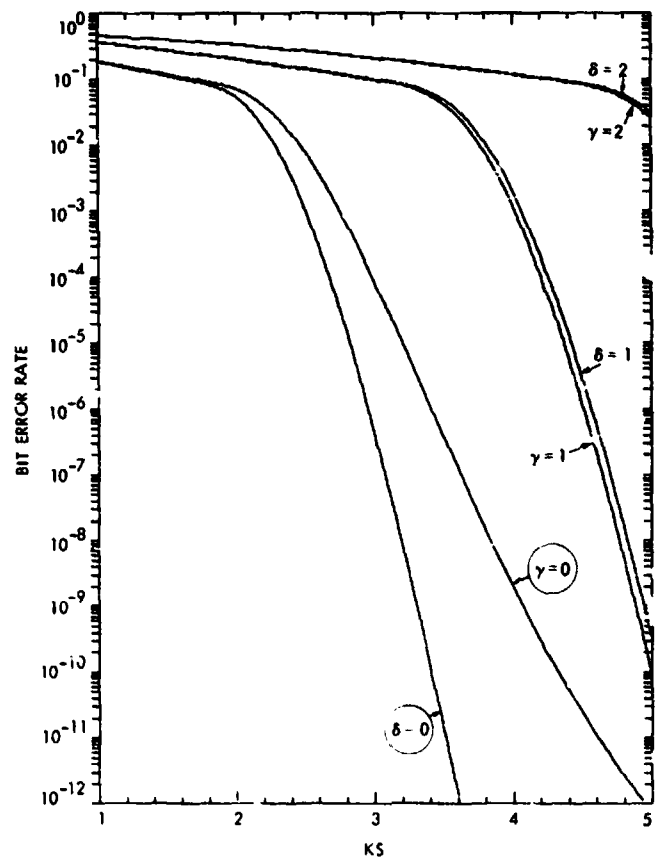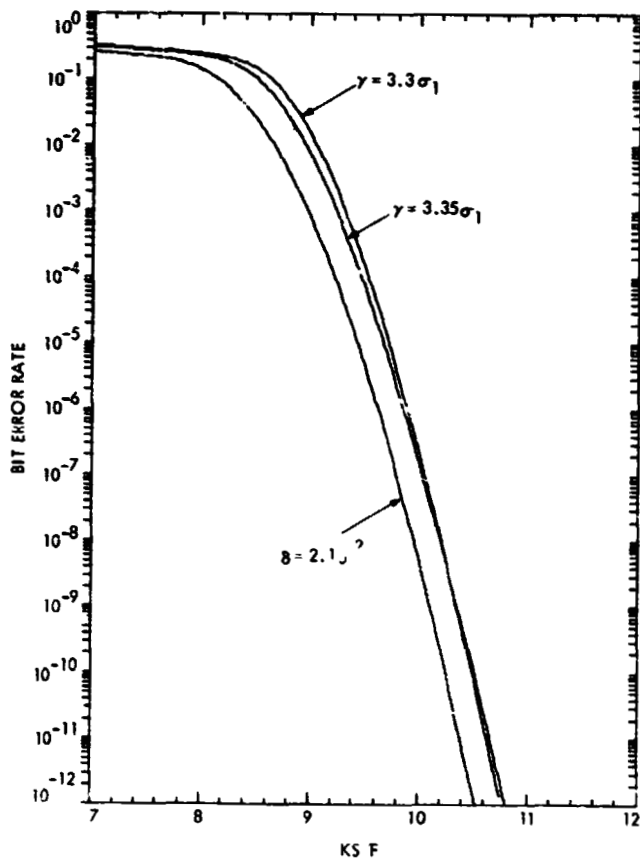Fig. 7. Bit error rate vs K_s for $K_b = 10^{-3}$ for RS (255, 223)

Fig. 8. Bit error rate vs K_s for $K_b = 10^{-4}$ for RS (255, 223)

Fig. 9. Bit error rate vs K_s/F for $K_b/F =$ ⁻. for RS (255, 127)

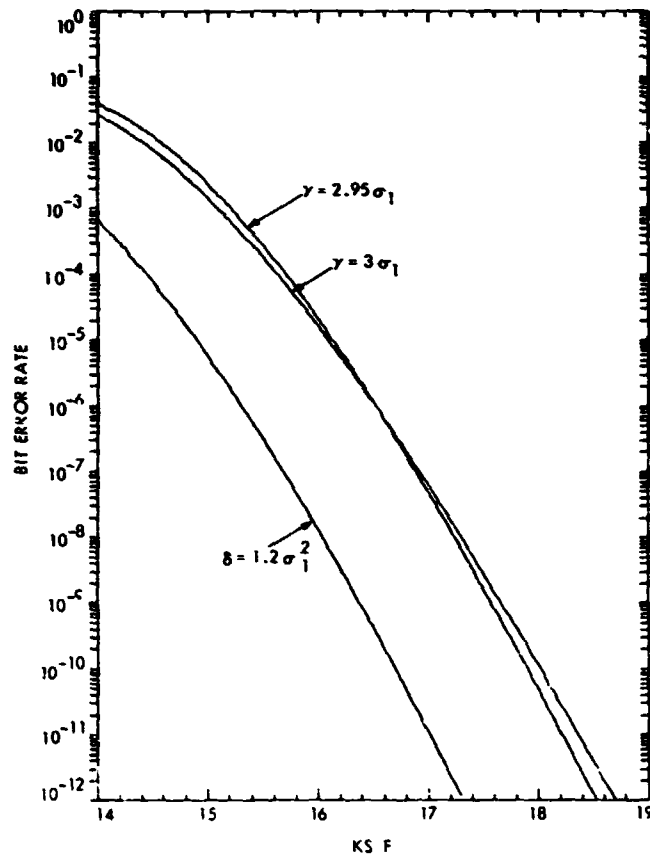**Fig. 10. Bit error rate vs K_s/F for $K_b/F = 5$ for RS (255, 191)**

Fig. 11. Bit error rate vs K_s/F for $K_b/F = 5$ for RS (255, 223)